EXPERIMENTAL INVESTIGATION OF THE PRESSURE LOSS THROUGH PERFORATED STRUCTURES IN UNSTEADY FLOW

L.J. Pedroso
R.J. Gibert

Rakenteiden Mekaniikka, Vol. 21
No 1 1988, 42...54

SUMMARY: The pressure drop associated with singularities in pipeworks in unsteady flow is considered. A parametric experimental approach, using a scale model, is adopted. The singularities consisted of perforated plates and diaphragms. A mathematical model was developed and experimental results were compared against it. The main conclusion was that for values of the parameter U_mT/d (the inverse of a Strouhal number) exceeding unity, the steady flow value for the singularity pressure drop coefficient can be taken, without risk of significant errors.

INTRODUCTION

Nuclear reactor circuits consists of pipework comprising certain singularities, such as pumps, valves, diaphragms, sharp changes in cross-section, elbows, permanent obstructions, etc...

The occurence of accidental transients (water hammer, depressurization, effects of a sodium-water reaction, ...) raises the following question:

How do the pressure waves propagate through the singularities? In this connection, it must be borne in mind that a damping effect will be induced by the pressure drop associated with the singularity.

The method used to answer this question consisted simply in extrapolating conventional results obtained for steady-state flows. But this lacks precision and can lead to errors.

With a view to solving this problem in a more satisfactory manner, we adopted a parametric experimental approach, using a scale model.

The singularities analyzed in the present survey are "flat singularities" (perforated plates and diaphrams).

TEST SETUP (RIO test rig)

The RIO test rig consists of a water-filled straight tube, 6.0 m in length, 8.5 cm in inside diameter, with a wall thickness of 8.0 mm. At the left -hand end of the tube, a piston connected to an electrohydraulic jack induces motion in the fluid inside the tube. At the other end, a pressurized tank with a free surface has been installed, to eliminate cavitation problems and minimize degassing effects.

Pressure transducers (piezoelectric) are mounted on the side of the tube, arranged at regular intervals, in a straight line, troughout its length. The "RIO" test rig is shown in diagram form in Figure 1.

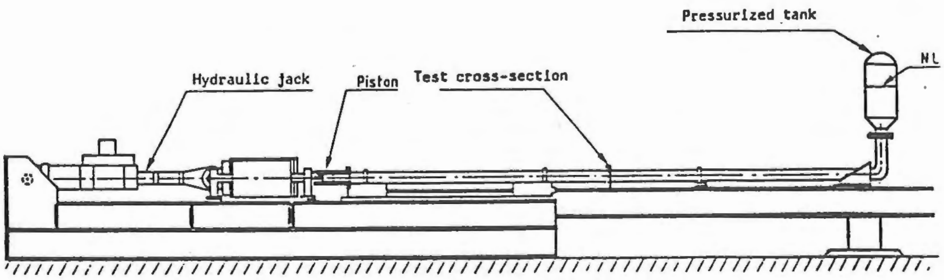

Figure 1. RIO test rig.

The test section is located approximately in the middle of the tube and is installed by means of two screw-on metal flanges, enabling the singularities under investigation to be inserted.

TEST PROCEDURE

As regards the singularities, we analyzed three different section porosities (0.05, 0.17 and 0.5), either with one hole (diaphragm) or with several holes, 8 mm in diameter.

The wall thickness is constant (e = 8.0 mm) (Fig. 2).

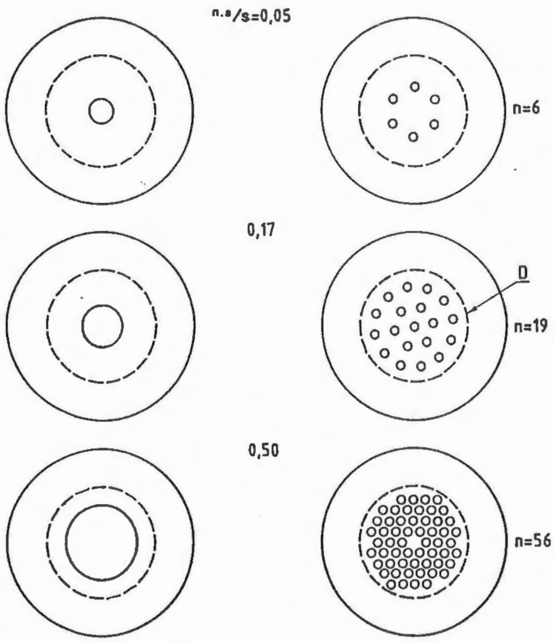

Figure 2. Singularities.

Each test consists in repeated sinusoidal sweeping, increasing in compass (frequency f = 2 to 20 Hz), for different piston displacement amplitudes (X_m = 2 to 30 mm). The two variables X_m and f are quantities limited by the maximum piston speed ($V_p = \omega X_m$ = 0.6 m/s).

It should be noted that the Reynolds number varies between 5×10^2 and 1.2×10^5.

The air in the pressurized tank is kept at a pressure of 3 bars and the water used has been degassed and demineralized, with an initial oxygen content of 10^{-2} ppm.

Measurement results are presented as time-dependency signals, power spectral densities, phase and modulus transfer functions, pressure profiles modulus along the tube.

GENERAL FORMULATION OF THE PROBLEM

Let us consider incompressible fluid motion in a straight horizontal tube of constant cross-section postulating a viscosity term represented by a pressure drop ΔP, characterized by a Reynolds dependent coefficient K ($K = \lambda(Re)/D_h$, where D_h is the hydraulic diameter of the tube, and λ the dimensionless friction coefficient). The governing one-dimensional equations are

$$Q = Q(t) \ , \tag{1}$$

$$\underbrace{\frac{\partial Q}{\partial t}\int_1^2 \frac{dx}{S}}_{\text{Inertia}} + \underbrace{\left[p + \frac{Q^2}{2\rho S^2}\right]_1^2}_{\Delta P_{1,2}} + \underbrace{\frac{Q^2}{2\rho}\int_1^2 \frac{K}{S^2}\,dx}_{\text{Pressure drop}} = 0 \tag{2}$$

where S is the cross-section, Q the mass flow rate and ρ the fluid density.

It is seen that the total pressure drop $\Delta P_{1,2}$ between two cross-section S_1 and S_2 is equal to the pressure drop induced by viscosity increased by the inertia effect associated with the acceleration of the fluid.

Integration of Singularities

By analogy with the tube having a constant cross-section (equa-

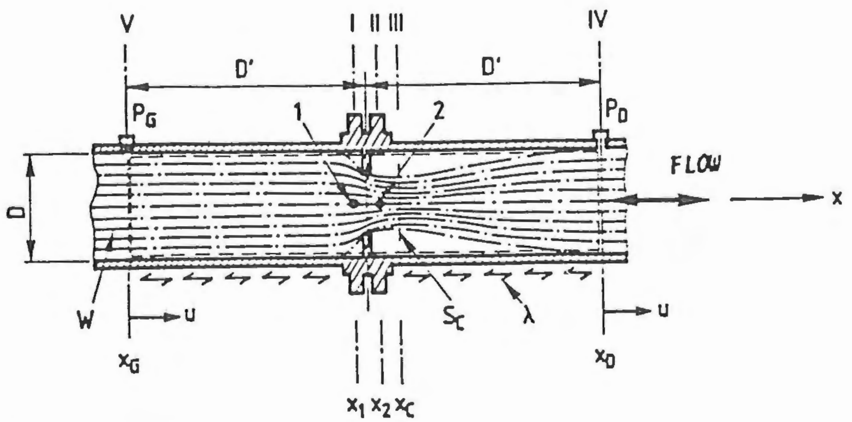

Figure 3. Zone with singularities.

tion (2)), the pressure drop $\Delta P_{1,2}$ at the boundaries of the segment containing singularities (Fig. 3) can be assumed to be represented by the sum of an inertia term (linear with respect to the mass flow rate) and a term representing dissipating effects (quadratic with respect to the mass flow rate):

$$\Delta P_{1,2} = \frac{\widetilde{\ell e}}{S} \frac{\partial Q}{\partial t} + K_s \frac{Q^2}{2\rho S^2} \tag{3}$$

where $\widetilde{\ell e} = e + \tilde{\ell}$; e is the length of the singularity.

a) The inertia term can be derived from the postulate assuming slightly incompressible fluid motion through the singularity. It is characterized by an equivalent length ℓe of a fictititious tube, having a constant cross-section s (singularity area), and where $\tilde{\ell}$ represents the 3-D effects in the vicinity of the singularity. This term can be determined by means of a calculation /1/.

b) The quadratic term can be determined by postulating a quasi-steady-state flow. The singularity pressure loss coefficient K_s is derived from conventional formulations to be found in technical literature. The purpose of our investigation is to confirm the validity of this assumption.

CALCULATION OF THE SINGULARITY PRESSURE DROP COEFFICIENT K_s UNDER OSCILLATING FLOW CONDITIONS

Since, at the singularity, the pressure drop phenomenon is not linear, the circuit response to harmonic piston motion is not sinusoidal and consequently comprises a set of harmonics deriving from the excitation frequency. Test result interpretation shall be based on the fundamental frequency. We then encounter the problem of deducing a certain pressure drop coefficient K_s. The following method can be used:

Let us take an oscillating flow, defined by

$$Q = -\rho S\, U_m \cos \omega t \;. \tag{4}$$

Here $U_m = \omega X_m$ is the maximum flow velocity and $\omega = 2\pi/T$ the angular frequency, where T is the oscillation period.

On the basis of a dimensional analysis, the singularity pressure drop term can be presented as follows

$$\frac{\Delta P_s}{U_m^2/2} = K(\theta, \frac{U_m T}{d}, \frac{U_m d}{\nu}, \frac{s}{S}, \frac{e}{d}) \qquad (5)$$

where $\theta = \omega t$, $U_m T/d$ is a period parameter = the inverse of a Strouhal number, $U_m d/\nu$ is the Reynolds number = R_e^s, d is the hole diameter and s is the hole cross-section.

The ratio K is a periodic function of θ, the fundamental frequency amplitude of which is K_1.

If we assume that K has a form of the type

$$\frac{\Delta P_s}{\rho U_m^2/2} = K_s \; |\cos\theta| \cos\theta \text{ (with } K_s \text{ constant)} \qquad (6)$$

we obtain

$$K_s = \frac{3\pi}{8} K_1 \qquad (7)$$

where K_s represents a mean pressure drop coefficient per cycle. It is this quantity that we shall derive from the test results.

APPLICATION OF THE MODEL TO THE RIO TEST RIG

In order to derive K_s from the pressure measurement results, we represent the test rig by the following model (Fig. 4).

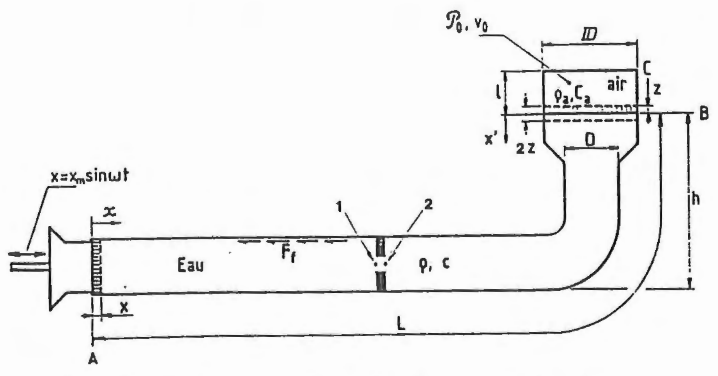

Figure 4. Physical model - RIO/pressurized.

We consider the column of liquid contained in a tube, of cross-section S.

At A the fluid is in contact with the harmonic drive piston $(X_m \sin \omega t)$ $(X_m \equiv x_o)$.

At B it is in contact with a layer of pressurized air.

We postulate that:

- the liquid is incompressible,
- motion is slight and one-dimensional,
- the special features (elbow, vertical pipe section, etc...) induce no significant effects,
- the gas behaviour is static throughout its volume,
- pressure fluctuations due to free level variations in the pressurized tank are disregarded.

It can be shown that the pressure field at any given point (upstream) on abscissa x is given by

$$P(x,t) = IP \,\mathrm{Sin}(\Theta-\varphi) \tag{8}$$

where

$$IP = \left|\underbrace{\left\{\frac{4}{3\pi}\rho U_m^2[K_s+K_f(L-x)]\right\}^2}_{\text{Pressure loss effects}} + \underbrace{\left\{-\rho\omega U_m\left[(L-x)+\frac{\widetilde{\ell e}}{\sigma}\right]}_{\text{Inertia effects}} + \underbrace{\gamma\,\varphi_o\,\frac{S}{\$}\,\frac{X_m}{\ell}\right\}^2}_{\text{Pressurization effects}}\right|^{\frac{1}{2}}, \tag{9}$$

$$\mathrm{tn}\,\varphi = \frac{4}{3\pi}\,\frac{\rho U_m^2[K_s+K_f(L-x)]}{\rho\omega U_m\left[(L-x)+\frac{\widetilde{\ell e}}{\sigma}-\gamma\,\varphi_o\,\frac{S}{\$}\,\frac{X_m}{\ell}\right]} \tag{10}$$

and where φ_o is the initial nominal pressurization, γ the gas constant, ℓ the length of pressurization tank, σ the cross-section ratio and $\$$ the pressurization tank cross-section.

For a point downstream from the obstacle, the pressure fields is given by the previous equations, but with K_s and $\widetilde{\ell e}$ equal to zero.

EXPERIMENTAL DETERMINATION OF THE PRESSURE DROP

The method to determine K_s for each test configuration consists of a fit between the experimental pressure profile and that obtained using equations (9) and (10) (Figs. 5a and 5b). In practice, errors of up to 100 % are observed for the small values of the parameter $U_m T/d$.

This is because in such cases the effects of inertia have a prevailing influence on the trend of the pressure field.

In the most favourble cases, the errors are below 10 %.

EXPERIMENTAL RESULTS

Figures 6a to 6d show the main results for singularity pressure drop coefficients, for two cross section ratios (σ = 0.05 and σ = 0.17), with one and with several holes.

The ratio between pressure drop coefficients under oscillating flow conditions K_s and under steady state conditions K_p /2/, is plotted versus $U_m T/d$.

It will be noted that the K_s-behaviour differs considerably from the K_p-behaviour.

K_s diminishes, at the outset, relatively fast and then gradually with $U_m T/d$.

Its final value is almost identical with that of K_p.

Generally speaking, within the limits of the values investigated, K_s exceeds K_p. Major differences are observed for the largest cross-section ratios. Also noteworthy are the scattered results obtained for low $U_m T/d$.

This is due to the measurement error previously mentioned, but, certainly, also to the fact that $U_m T/d$ is not the only parameter affecting the problem (see equation (5)). The Reynolds number varies considerably from one experimental point to another.

CONCLUSIONS

The main conclusion of this survey is that for values of the parameter $U_m T/d$ exceeding unity, the steady flow value for the singularity pressure drop coefficient can be taken, without risk of significant errors. This limit value of $U_m T/d$ tends to increase in cases where the cross-section ratios are large.

In the case of small $U_m T/d$ values, the dispersion effect with

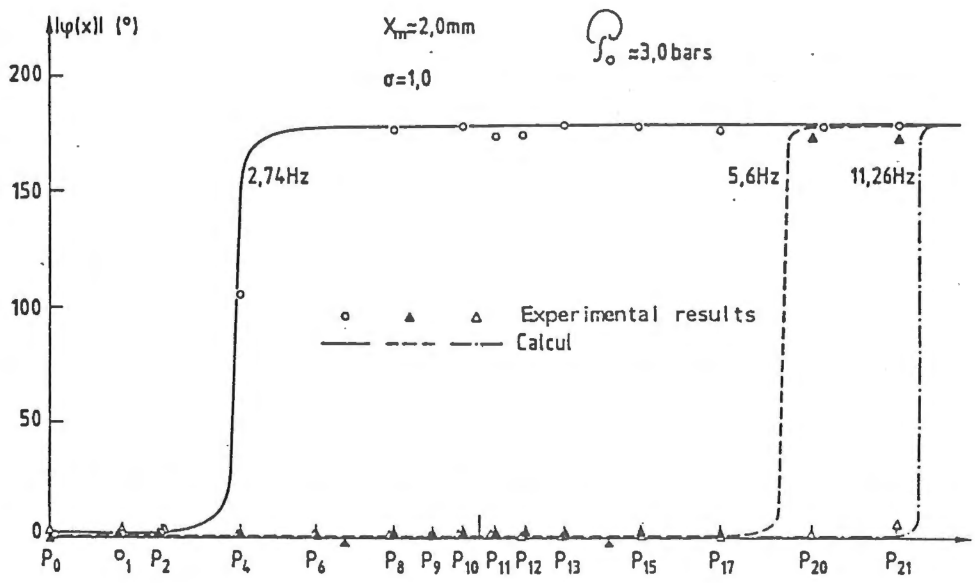

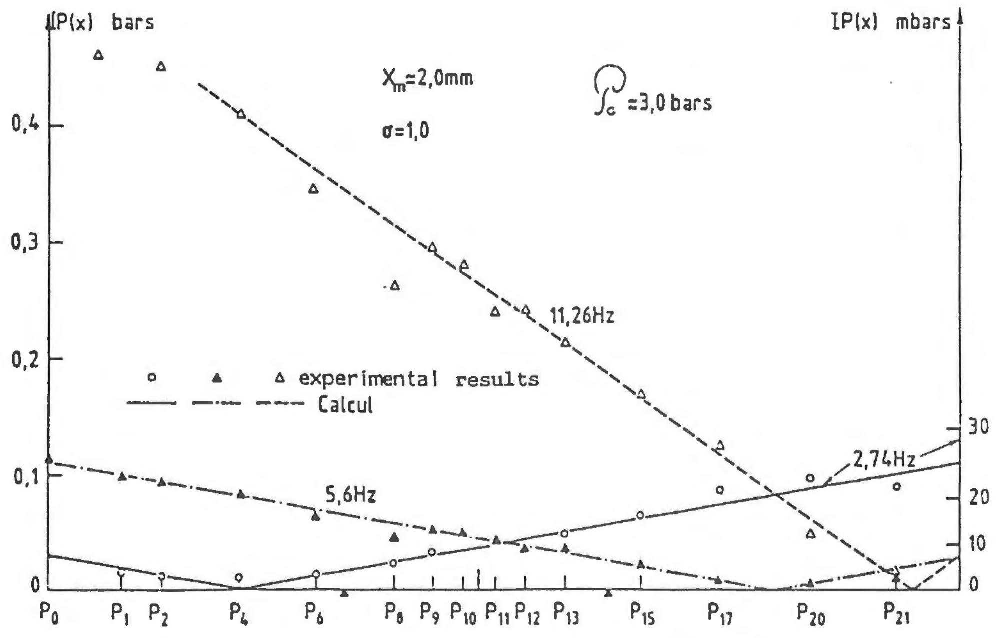

Figure 5a. Phase shift and pressure profile versus frequency (tube without singularities).

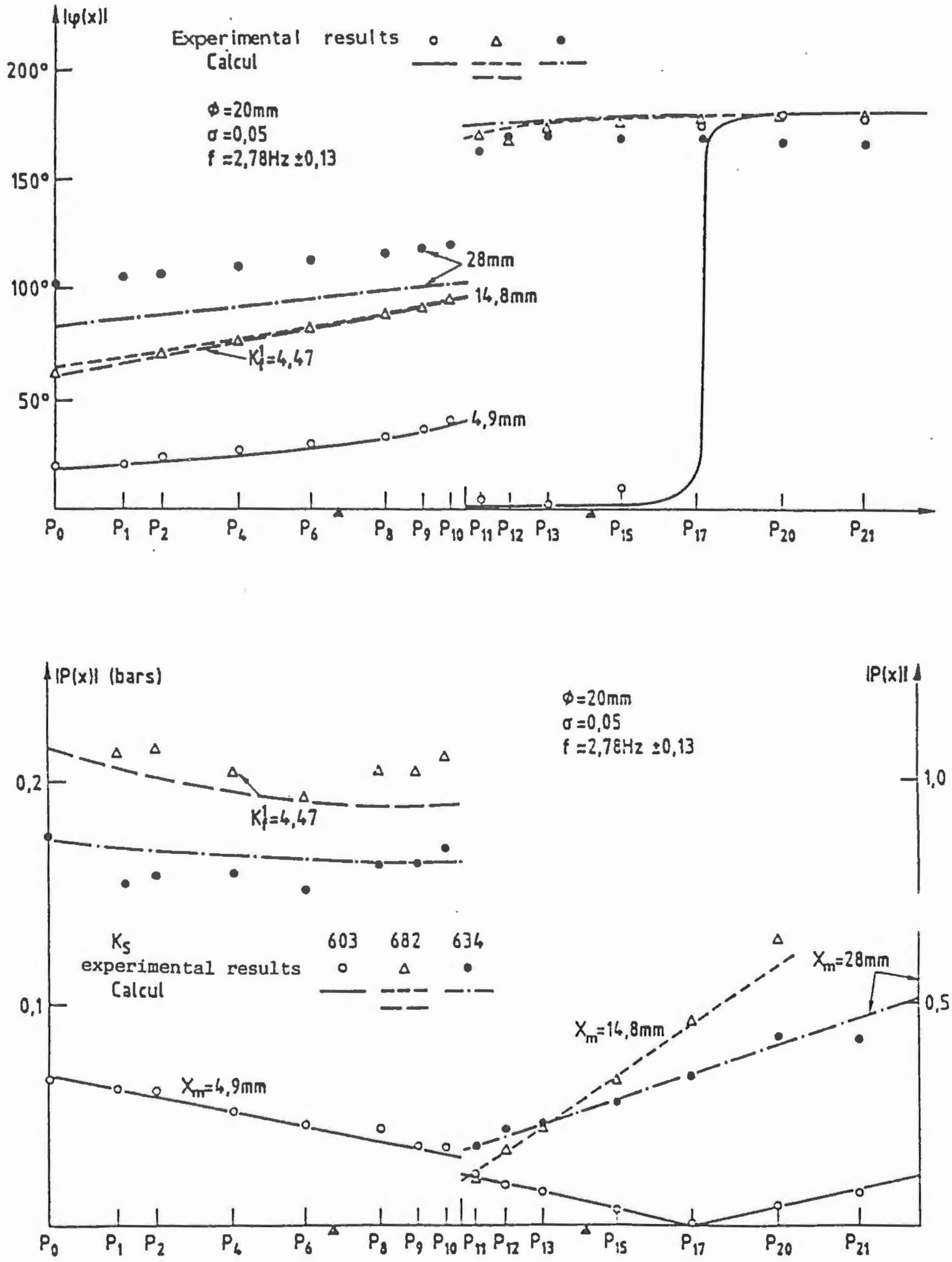

Figure 5b. Phase shift and pressure profile versus piston motion (tube with singularities).

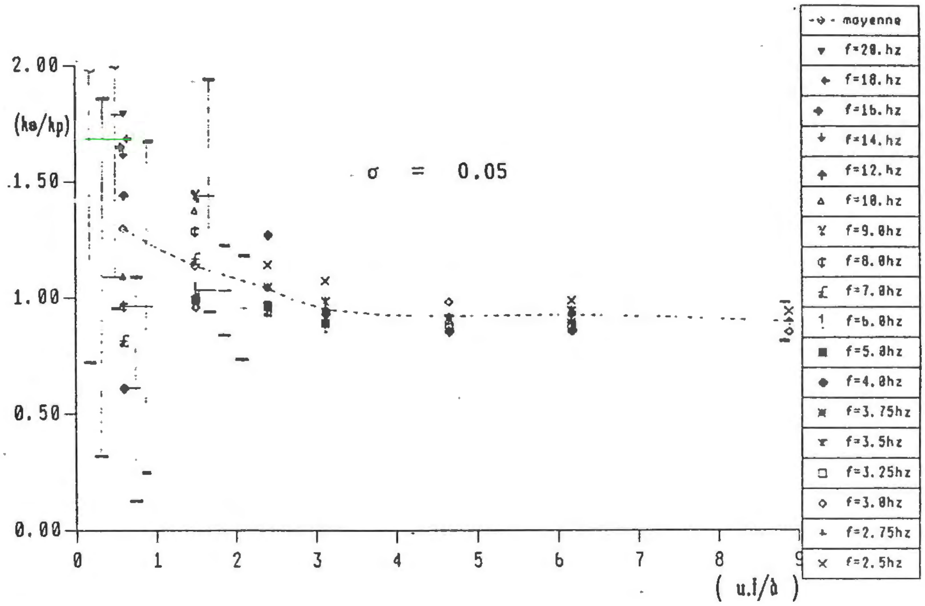

Figure 6a. Variation of the ratio (k_s/k_p) versus period parameter for several frequencies (1×20 mm).

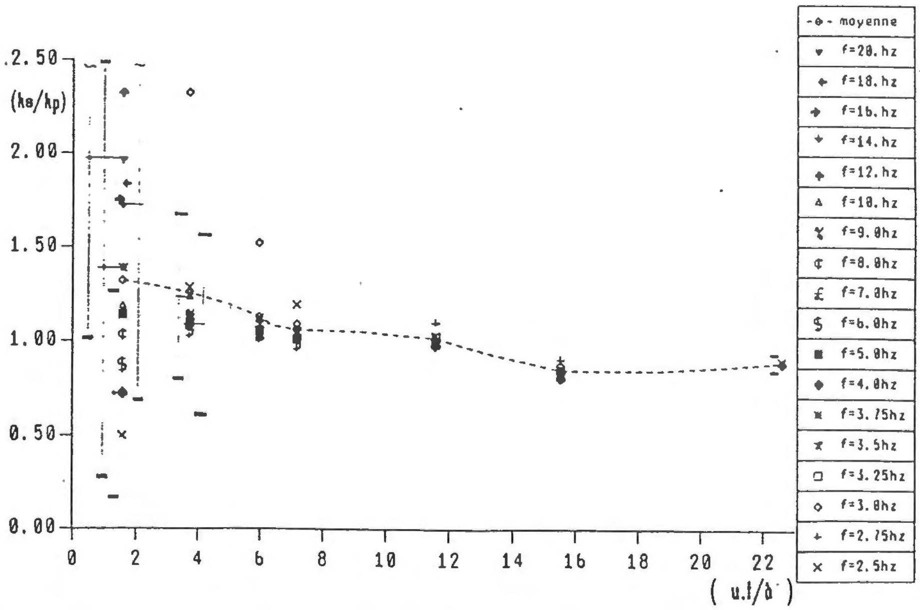

Figure 6b. Variation of the ratio (k_s/k_p) versus period parameter for several frequencies (6×8 mm).

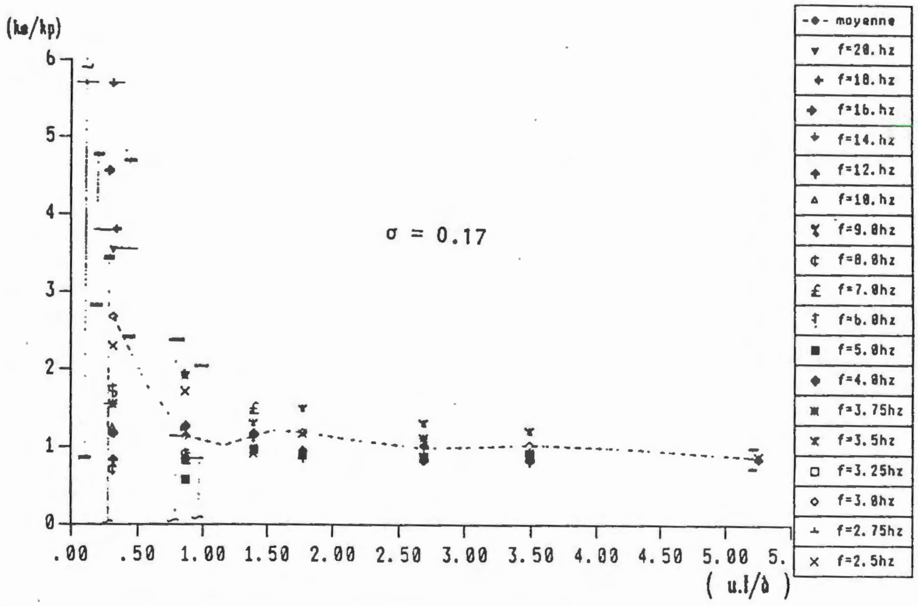

Figure 6c. Variation of the ratio (k_s/k_p) versus period parameter for several frequencies (1×35 mm).

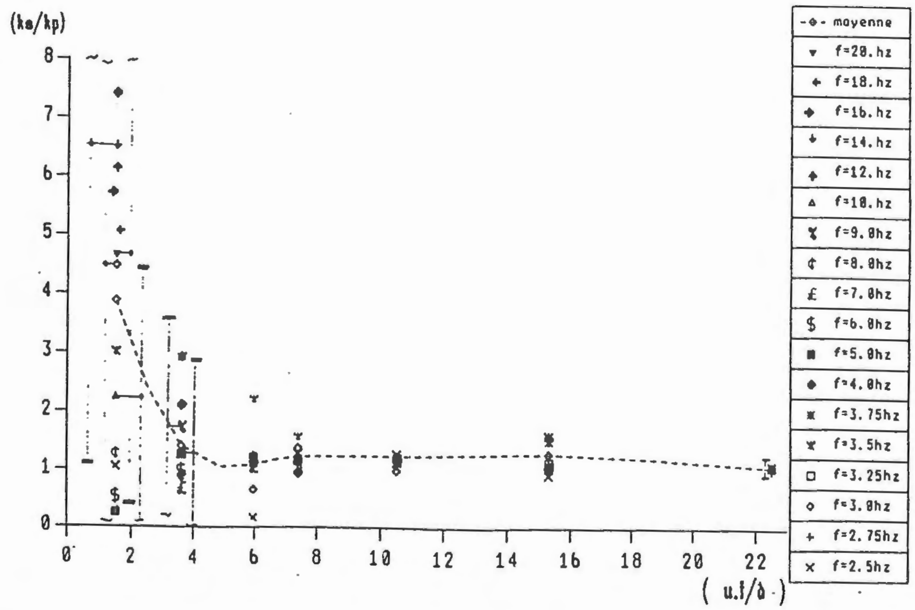

Figure 6d. Variation of the ratio (k_s/k_p) versus period parameter for several frequencies (19×8 mm).

respect to K_s would appear to be significant, but, owing to measurement errors, it is difficult to determine the relative influence of U_mT/d and the Reynolds number.

However, it must be remembered that, in these cases, pressures drop effects are slight as compared with inertia effects.

REFERENCES

[1] Durandet, E.; Gibert, R.J., Effects of Fluid Communications between Fluid Volumes on the Seismic Behaviour of Nuclear Breeder Reactor Intervals to be presented at 9th SMIRT, Lausanne, Aug. 17.21, 1987.

[2] Idel'cik, J.E., Mémento des pertes de charge, Eyrolles, Paris 1986.

[3] Pedroso, L.J., Qualification expérimentale des méthodes de calculs des interactions fluide-structure dans les circuits tubulaires des réacteurs nucléaires, Thése de Doctorat, INSTN/ DEMT, CEA, Saclay, 1986.

[4] Matten, R.B., The Influence of Surface Roughness upon the Drag of Circular Cylinders in Waves, In: Off-shore Technologie Conference OTC 2902, pp. 185 - 194, May 1977.

[5] Sarpkaya, T., Forces on Cylinder and Spheres in a Sinusoidal Oscillating Fluids, J. of Appl. Mech., Trans. of the ASME, May 1975, pp. 32-37.

[6] Sarpkaya, T., Forces on Cylinder near a Plane Boundary in a Sinusoidal Oscillating Fluid, J. of Fluids Eng., Trans. of the ASME, Sept. 1976, pp. 499-505.

[7] Susbielle, G. et Bratu, C., Vagues et ouvrages pétroliers en mer, Publication de l'IFP, Editions Technip, Paris, 1981.

[8] Hogben, N. et al., Estimation of Fluid Loading of Off-shore Structures, Proc. Inst. Civil Engs., part 2, pp. 512-562, 1977.

[9] Bushnell, M.J., Forces on Cylinder Arrays in Oscillating Flow, In: Off-shore Technology Conference; OTC 2903, May 1977; p. 193.

[10] Paape, A. and Breuseurs, H.N.C., The Influence of Pile Dimensions on Forces Excerted by Waves, DELFT Hydraulics Laboratory, Publication no 41, Oct. 1966.

L.J. Pedroso, R.J. Gibert, Commissariat A l'Energie Atomique, Division d'Etude et de Developpement des Reacteurs Departement des Etudes Mecaniques et Thermiques Laboratoire des Vibrations et Seismes, Centre d'Etudes Nucléaires de Saclay, 91191 Gif s/Yvette Cedex, FRANCE